Physical properties of galaxies through cosmic time

E.-D. Paspaliaris[1,2], M. Xilouris[1] & A. Nersesian[1,3]

1. Institute for Astronomy, Astrophysics, Space Applications & Remote Sensing, National Observatory of Athens
2. Department of Astrophysics, Astronomy & Mechanics, School of Physics, Aristotle University of Thessaloniki
3. Department of Astrophysics, Astronomy & Mechanics, Faculty of Physics, University of Athens

Abstract:

Recently, *Nersesian et al. (2019)* investigated the different stellar population mixes in nearby galaxies (DustPedia sample; *Davies et al. 2017*) and their role in dust heating. In the current study we make use of a sample of ~90 local (U)LIRGs (*Papadopoulos et al. 2012; Greve et al. 2014*), occupying the high end of SFR in the local Universe, as well as galaxies at higher redshifts (HELP sample; *Vaccari et al. 2016*) aiming at linking the properties of local and distant galaxies and examining their evolution through cosmic time. We make use of multi-wavelength photometric data (from the UV to the submm) already culled in the databases mentioned above and the CIGALE SED fitting tool to investigate the role of dust and its heating by radiation, due to different stellar populations, on the variances of several parameters for galaxies of different morphological types and merging stages.

SED-fitting

Figure 1. Template SEDs for three main types of galaxies [Early-type (ETGs), Late-type (LTGs), and (U)LIRGs] as derived by CIGALE. The median SED of each sub-class is shown as a white curve; the unattenuated SEDs of the old and the young stars are shown as red and blue curves, respectively. The orange curve indicates the median spectrum of the diffuse dust, while the green curve the emission from PDRs. The purple curve indicates the 75th percentile of the median spectrum of the emission by the AGN. The shaded areas cover the range of the 16–84th percentiles to the median value.

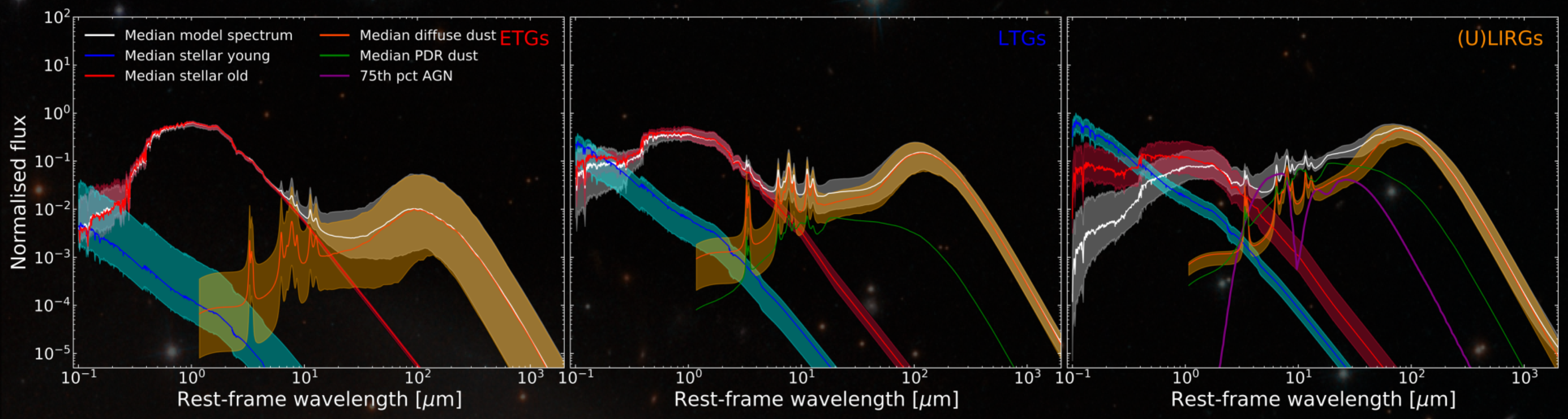

Results

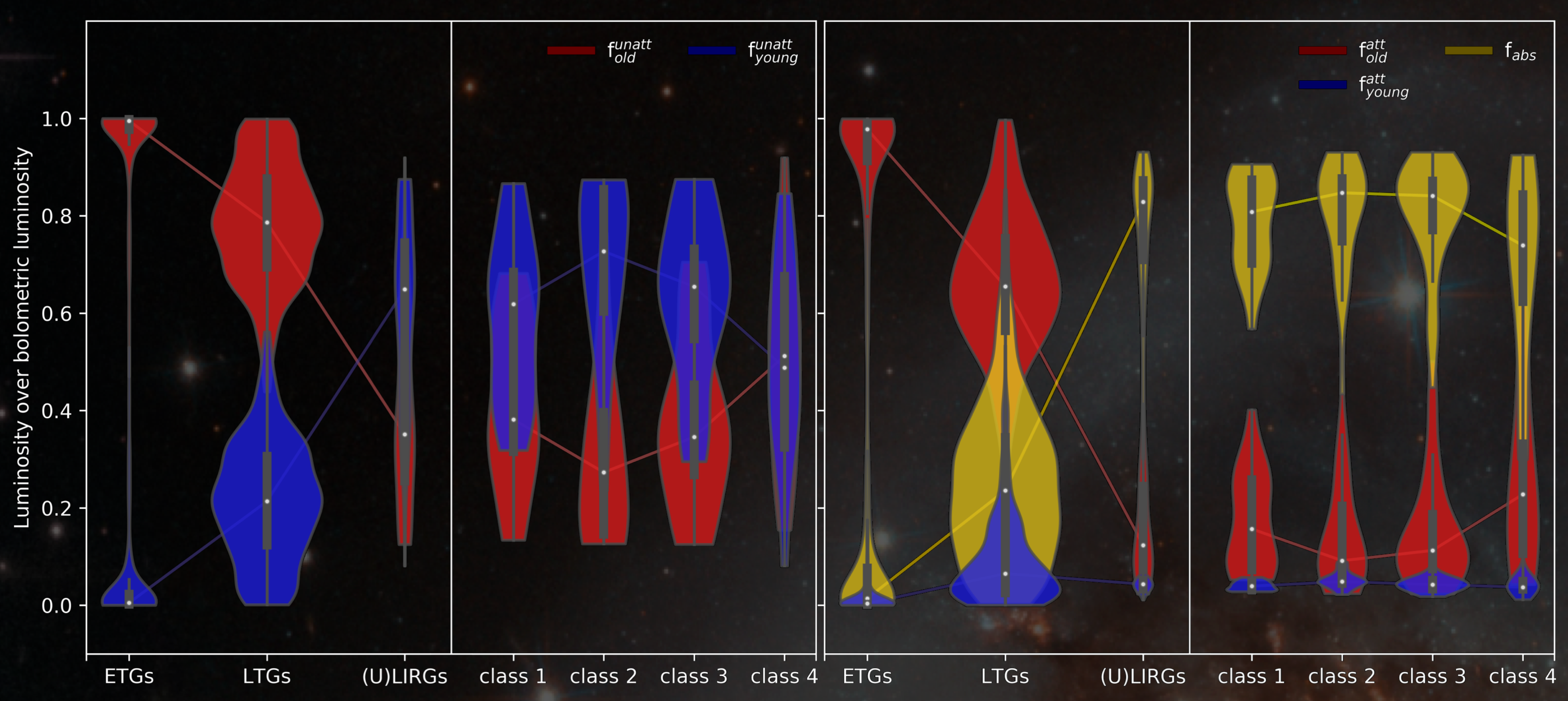

Figure 3. Left panel: The contribution of the old (red) and the young (blue) stellar populations to the unattenuated luminosity, over the bolometric luminosity Right panel: The contribution of the old and the young stellar populations to the attenuated luminosity, over the bolometric luminosity, together with the ratio of the dust luminosity to the bolometric luminosity (f_{abs} ; yellow).

White dots indicate the median values, for each specific galaxy type and merging class. The thick dark-gray bar represents the interquartile range and the thin dark-gray line in the center represents the rest of the distribution. The colored area, confined by the dark-gray border, shows the distribution shape of the data, derived by a kernel density estimation.

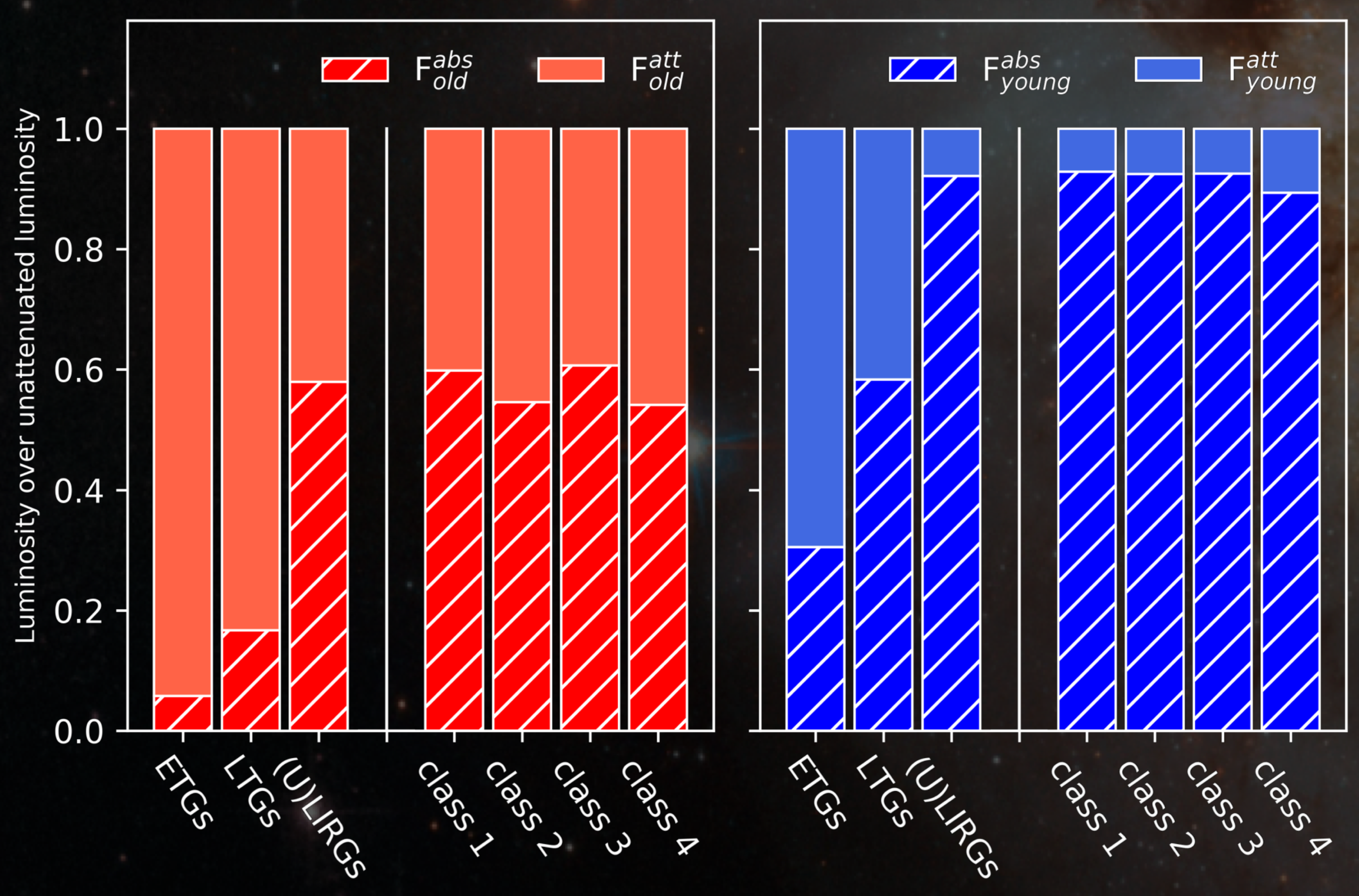

Figure 4. Mean values of the portion of the luminosity of the old and young stellar populations (left and right panel, respectively) used for the heating of the dust. The dashed bars stand for the mean values of the ratio of the absorbed by dust luminosity, to the unattenuated luminosity by the corresponding stellar component. The mean values of the ratio of the attenuated luminosity of the specific stellar component to the unattenuated luminosity are indicated as filled bars.

Figure 5. The luminosity of the different dust components per galaxy type and per (U)LIRG merging class. Green markings represent the PDR dust luminosity, orange stand for the luminosity of the diffuse dust, while the total dust luminosity is in gray. Median values are indicated with square symbols.

(U)LIRGs classification

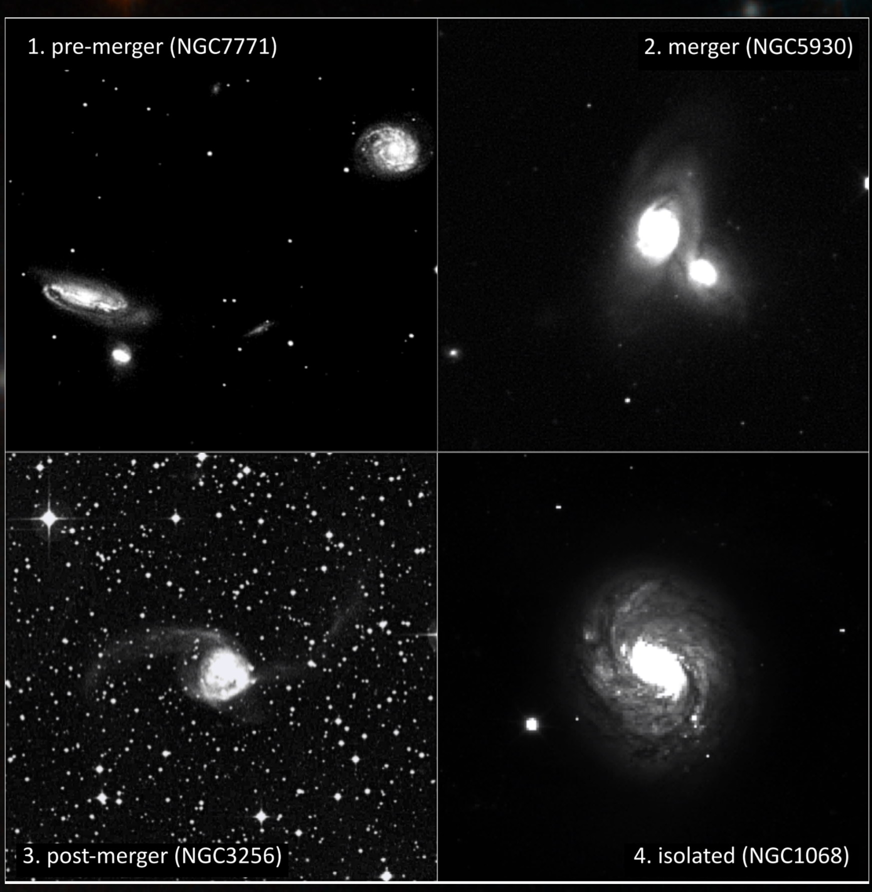

Figure 2. Indicative optical images of the different merging stages of (U)LIRGs in our sample.

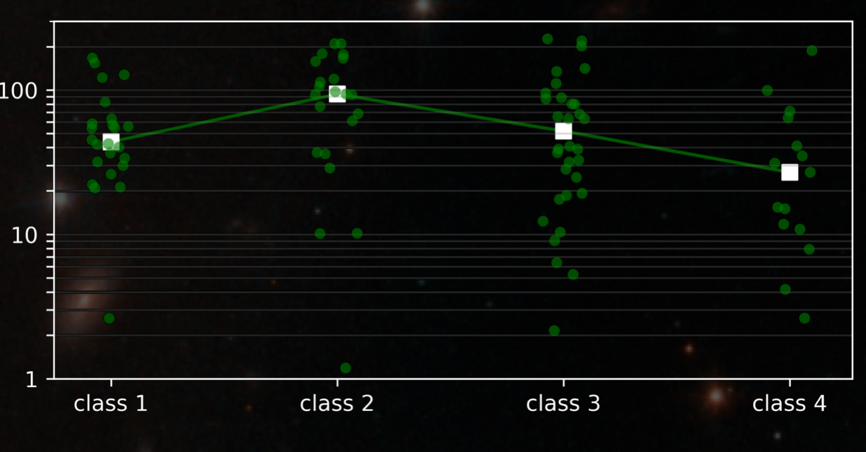

Figure 6. Star formation rates of (U)LIRGs in different merging stages, as derived from CIGALE. Green circles correspond to individual systems, while the white squares stand for the median values per merging class.

* Conclusions *

- *interacting (U)LIRGs form new stars with a higher - by a factor of ~2 - rate than the isolated (U)LIRGs. This finding agrees with previous observational studies and simulations. Additionally their SFR is an order of magnitude higher than in normal galaxies.*
- *Most of the energy emitted by both stellar populations (old and young) in (U)LIRGs is offered for the dust heating. The young stellar population is, in all galaxy types, more efficient in heating the dust. Its highest contribution is observed in class 2 (U)LIRGs, where it is 79 %, on average.*
- *Although it is unclear if the SFR has any correlation with the stellar mass for (U)LIRGs, they cover an area in the main sequence diagram that is also occupied by higher-z sources.*
- *In very luminous IR-galaxies, not only the AGN emission, but also the emission of the PDR dust can determine the shape of the MIR region of the galaxy spectrum; especially in galaxies with weak or intermediate AGN activity.*

Towards higher redshifts...

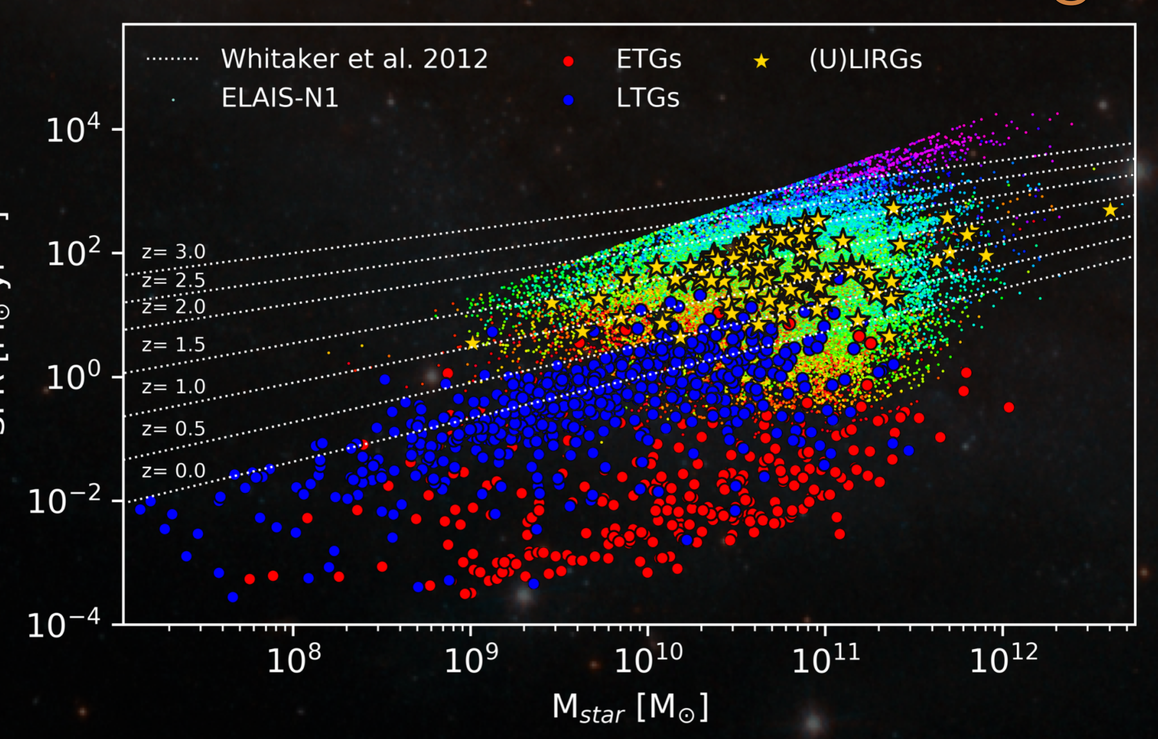

Figure 7. The main sequence (M_{star} vs SFR) of local normal galaxies [ETGs (red circles) and LTGs (blue circles)], local (U)LIRGs (yellow stars) and high-redshift galaxies (small dots color-coded according to redshift [see the vertical color-bar in Fig. 8)]. The white dotted lines correspond to the power law relations presented in *Whitaker et al. (2012)* for the redshift values indicated in the plot.

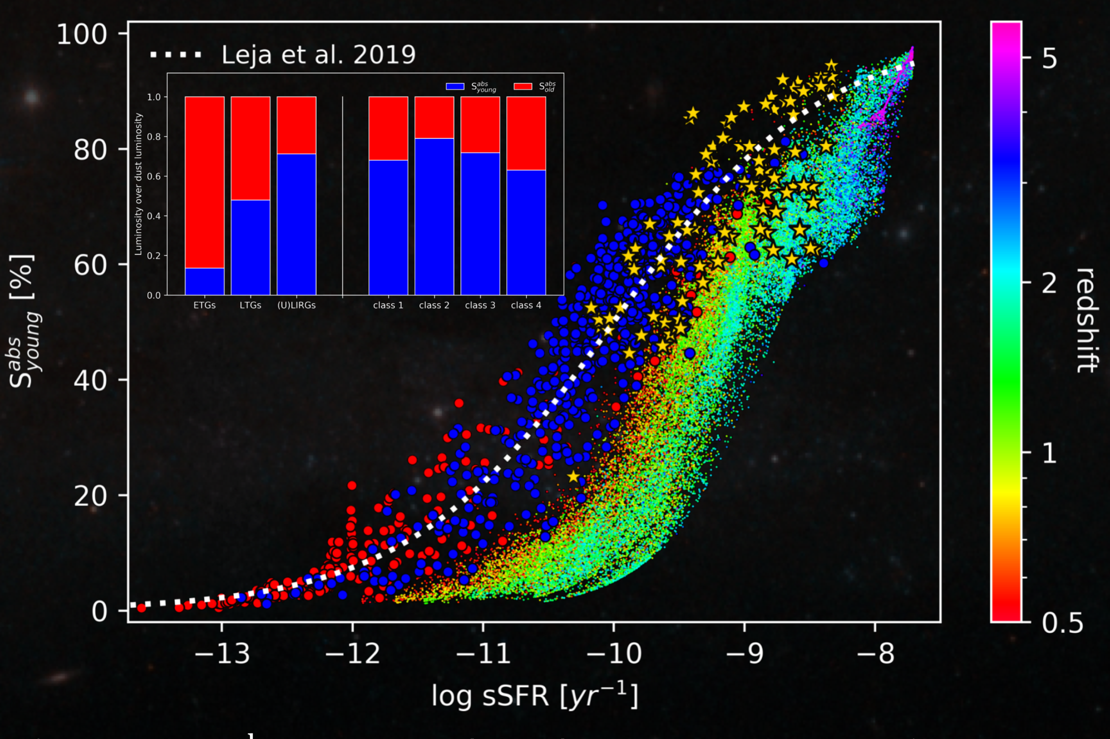

Figure 8. S^{abs}_{young} vs log(sSFR). The dotted white curve indicates the relation presented in *Leja et al. (2019) fitted* to the DustPedia galaxies. A smooth transition of ratios of the luminosity absorbed by dust (S^{abs}_{young}), from local to higher-redshift galaxies (of higher sSFR), with a similar S-shaped form, is evident. The inset plot indicates the mean values of the $S^{abs}_{old,young}$ for each (local) galaxy type. Red and blue bars refer to the old and the young stars, respectively.

References:

Bianchi, S., De Vis, P., Viaene, S., et al. 2018, A&A, 620, A112
Boquien, M., Burgarella, D., Roehlly, Y., et al. 2019, A&A, 622, A103
Davies, J. I., Baes, M., Bianchi, S., et al. 2017, PASP, 129, 044102
Greve , T. R., Leonidaki, I., Xilouris, E. M., et al. 2014, ApJ, 794, 142
Leja, J., Johnson, B. D., Conroy, C., et al. 2019, ApJ, 877, 140
Nersesian, A., Xilouris, E. M., Bianchi, S., et al. 2019, A&A, 624, A80
Whitaker, K. E., van Dokkum, P. G., Brammer, G., et al. 2012b, ApJ, 754, L29
Vaccari, M. 2016, The Universe of Digital Sky Surveys, 42, 71
Papadopoulos, P. P., van der Werf, P., Xilouris, E. M., et al. 2012, ApJ, 751, 10